International Journal of Mechanical, Industrial and Aerospace Sciences
ISSN: 2517-9950
Vol:12, No:2, 2018

Flow Analysis of Viscous Nanofluid Due to Rotating Rigid Disk with Navier's Slip: A Numerical Study

Khalil Ur Rehman, M. Y. Malik, Usman Ali

***Abstract*—**In this paper, the problem proposed by Von Karman is treated in the attendance of additional flow field effects when the liquid is spaced above the rotating rigid disk. To be more specific, a purely viscous fluid flow yield by rotating rigid disk with Navier's condition is considered in both magnetohydrodynamic and hydrodynamic frames. The rotating flow regime is manifested with heat source/sink and chemically reactive species. Moreover, the features of thermophoresis and Brownian motion are reported by considering nanofluid model. The flow field formulation is obtained mathematically in terms of high order differential equations. The reduced system of equations is solved numerically through self-coded computational algorithm. The pertinent outcomes are discussed systematically and provided through graphical and tabular practices. A simultaneous way of study makes this attempt attractive in this sense that the article contains dual framework and validation of results with existing work confirms the execution of self-coded algorithm for fluid flow regime over a rotating rigid disk.

***Keywords*—**Nanoparticles, Newtonian fluid model, chemical reaction, heat source/sink.

I. Introduction

THE magnetohydrodynamics (MHD) is the study of interaction of fluids with magnetic field while flowing through externally applied magnetic field. The varying properties of fluid flow regime manifested with different physical effects are difficult to narrate as an absolute feature. Therefore, various artificial techniques are suggested and carried out to depict the complete description of boundary layer characteristics. The application of MHD is one the important methods to avoid frequent movement of particles being source of turbulence. Beside this, the role of MHD is significant in various fields like in solar physics, revolving magnetic stars, and solar cycle to mention just a few. To be more specific, in early 1960s, researchers [1] pointed the significance of MHD boundary layer flows in the context of engineering and industrial applications namely MHD power generators, nuclear reactors, extrusion, metallurgical enrolments, significant performance in the field of plasma, petroleum individualities and energy extraction processes in geothermal science. Therefore, analysis on MHD flows admits received massive attention by researches; like in 1979, Chakrabarti and Gupta [1] discussed the MHD characteristics along with heat transfer towards flat surface. In 1995, the exact solution of Navier-Stokes equations in the presence of magnetic field effects was given by Andersson [2]. In 1998, the flow field properties in the presence of magnetic force towards porous media were studied by Pop and Na [3] while in 2003, Liao [4] contributed to analytic solution of non-Newtonian fluids flow due to flat stretching surface under the region of applied magnetic field. This work was very helpful for researchers to encounter the effects of magnetic field subject to Newtonian fluid models. In 2009, following the work of Liao [4], the MHD effects were considered in viscos fluid flow over a shrinking surface with the aid of homotopy analysis method (HAM). The exact values of viscous fluid towards flat surface in the presence of magnetic and slip effects were presented by Fang et al. [6] in 2009. In addition, in the same year, the closed form solution subject to Newtonian fluid flow under the influence of magnetic field was proposed by Fang and Zhang [7]. The advanced transform scheme is present by Rashidi [8], in the same year, to solve MHD boundary layer equations. The effects of magnetic field on viscous flow subject to non-linear surface were discussed by Ghotbi [9] by means of HAM. Kumaran et al. [10] discussed the exact solution of MHD flow of viscous fluid due to quadratically stretching surface. The numerical solution of MHD fluid flow under the region of stagnation point was reported by Ishak et al. [11]. In 2010, the transition effects because of applied magnetic field were analysed numerically on Newtonian fluid flow due to stretching flat surface by Kumaran et al. [12], while the non-perturbative solution of MHD Newtonian fluid flow over a shrinking surface was given by Noor et al. [13]. In 2011, the pressure variations in Newtonian fluid flow the presence of magnetic field were discussed by Tamizharasi and Kumaran [14].

The applications of fluid flow due to rotation of solid surfaces include crystal growth processes, gas turbine rotors and thermal power generation system. These type of involvements via rotating disk are widely recognized by researchers and scientist, namely in 2006, Yang and Liao [15] proposed analytic solution von Karman swirling viscous flow while in 2007, Asghar et al. [16] studied MHD fluid flow due to accelerated disk. In 2008, Attia [17] discussed heat transfer properties on porous rotating disk with non-Newtonian fluid model. In 2009, Rashidi and Shahmohamadi [18] proposed analytical solution of Navier-Stokes equations for fluid flow due to rotating disk while in 2011, Devi and Devi [19] identified Dufour and Soret effects on slip flow due to porous rotating disk. In 2012, Dandapat and Singh [20] discussed unsteadiness effect in two-layer film flow on rotating disk while in 2013, Turkyilmazoglu and Senel [21] discussed numerical solution of fluid flow due to rotating disk along

Khalil Ur Rehman is with the Department of Mathematics, Quaid-i-Azam University Islamabad 44000, Pakistan (corresponding author, phone: +92336-5535137; e-mail: krehman@math.qau.edu.pk).

M. Y. Malik and Usman Ali are with the Department of Mathematics, Quaid-i-Azam University Islamabad 44000, Pakistan.

with both heat and mass transfer characteristics. Recently, Hayat et al. [22] discussed Navier's slip effects on viscous fluid flow induced by rotating solid disk.

The key purpose of present work is to report comparative analysis of purely viscous nanofluid flow due to rotating rigid disk with Navier's slip condition for MHD and hydrodynamic cases. The flow field formulation is carried out in the presence of heat source/sink and chemically reactive species, while the mutual interaction of thermophoretic and Brownian motion phenomena is acknowledged by considering nano-size particles. The article is designed in such a way that the Section I is all about literature survey subject to pertinent physical assumptions that are carried in present develop problem. Section II is devoted for mathematical formulation by means of fundamental rheological laws used in the field of continuum mechanics. To obtain numerical solution, a computational algorithm is established for present flow problem and its basic substitution practice is highlighted in Section III. The impact of involved parameters and physical numbers are discussed in Section IV and presented by way of graphical outcomes in Section V. Afterwards, the observations based on viscous nanofluid flow brought by solid rotating disk along with Navier's slip condition, heat source/sink and chemical reaction phenomena in both MHD and hydrodynamic frame are summarized in terms of closing remarks as a Section VI.

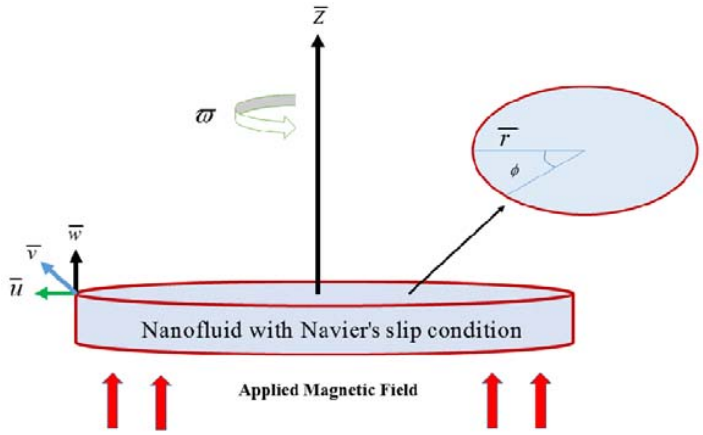

Fig. 1 Geometrical illustration of flow model

II. Mathematical Formulation

The viscous nanofluid flow yield by rotating rigid disk is considered along with velocity slip condition. The uniform magnetic field with strength B_0 is applied in the direction of $\bar{z}-axis$, while the assumption of small magnetic Reynolds number allows us to neglect induced magnetic field. The disk at $\bar{z}=0$ is rotating constantly with an angular velocity $\bar{\Omega}$. The effects of heat source/sink and chemically reactive species are taken into account. The velocity component $\bar{u}$ is in the $\bar{r}$ -direction, $\bar{v}$ is in the $\bar{\phi}$ -direction and $\bar{w}$ is in the $\bar{z}$ -direction. The flow narrating differential equations are written as:

$$\frac{\partial \bar{w}}{\partial \bar{z}}+\frac{\partial \bar{u}}{\partial \bar{r}}+\frac{\bar{u}}{\bar{r}}=0, \tag{1}$$

$$\bar{w}\frac{\partial \bar{u}}{\partial \bar{z}}+\bar{u}\frac{\partial \bar{u}}{\partial \bar{r}}-\frac{\bar{v}^2}{\bar{r}}=\nu\left(\frac{\partial^2 \bar{u}}{\partial \bar{z}^2}+\frac{1}{\bar{r}}\frac{\partial \bar{u}}{\partial \bar{r}}+\frac{\partial^2 \bar{u}}{\partial \bar{r}^2}-\frac{\bar{u}}{\bar{r}^2}\right)-\frac{\sigma {B_0}^2}{\rho_f}\bar{u}, \tag{2}$$

$$\bar{w}\frac{\partial \bar{v}}{\partial \bar{z}}+\bar{u}\frac{\partial \bar{v}}{\partial \bar{r}}+\frac{\bar{u}\bar{v}}{\bar{r}}=\nu\left(\frac{\partial^2 \bar{v}}{\partial \bar{z}^2}+\frac{\partial^2 \bar{v}}{\partial \bar{r}^2}-\frac{\bar{v}}{\bar{r}^2}+\frac{1}{\bar{r}}\frac{\partial \bar{v}}{\partial \bar{r}}\right)-\frac{\sigma {B_0}^2}{\rho_f}\bar{v}, \tag{3}$$

$$\bar{w}\frac{\partial \bar{w}}{\partial \bar{z}}+\bar{u}\frac{\partial \bar{w}}{\partial \bar{r}}=\nu\left(\frac{\partial^2 \bar{w}}{\partial \bar{z}^2}+\frac{1}{\bar{r}}\frac{\partial \bar{w}}{\partial \bar{r}}+\frac{\partial^2 \bar{w}}{\partial \bar{r}^2}\right), \tag{4}$$

$$\bar{w}\frac{\partial \bar{T}}{\partial \bar{z}}+\bar{u}\frac{\partial \bar{T}}{\partial \bar{r}}=\alpha\left(\frac{\partial^2 \bar{T}}{\partial \bar{z}^2}+\frac{1}{\bar{r}}\frac{\partial \bar{T}}{\partial \bar{r}}+\frac{\partial^2 \bar{T}}{\partial \bar{r}^2}\right)+\frac{(\rho c)_p}{(\rho c)_f}\left[D_B\left(\frac{\partial \bar{T}}{\partial \bar{z}}\frac{\partial \bar{C}}{\partial \bar{z}}+\frac{\partial \bar{T}}{\partial \bar{r}}\frac{\partial \bar{C}}{\partial \bar{r}}\right)\right]+\frac{(\rho c)_p}{(\rho c)_f}\left[\frac{D_T}{\bar{T}_\infty}\left(\left(\frac{\partial \bar{T}}{\partial \bar{z}}\right)^2+\left(\frac{\partial \bar{T}}{\partial \bar{r}}\right)^2\right)\right]+\frac{Q_0}{c_p\rho}\left(\bar{T}-\bar{T}_\infty\right), \tag{5}$$

$$\bar{w}\frac{\partial \bar{C}}{\partial \bar{z}}+\bar{u}\frac{\partial \bar{C}}{\partial \bar{r}}=D_B\left(\frac{\partial^2 \bar{C}}{\partial \bar{z}^2}+\frac{1}{\bar{r}}\frac{\partial \bar{C}}{\partial \bar{r}}+\frac{\partial^2 \bar{C}}{\partial \bar{r}^2}\right)+\frac{D_T}{\bar{T}_\infty}\left[\frac{\partial^2 \bar{T}}{\partial \bar{z}^2}+\frac{1}{\bar{r}}\frac{\partial \bar{T}}{\partial \bar{r}}+\frac{\partial^2 \bar{T}}{\partial \bar{r}^2}\right]-R_0\left(\bar{C}-\bar{C}_\infty\right), \tag{6}$$

$$\bar{u}=L\frac{\partial \bar{u}}{\partial \bar{z}},\bar{v}=\bar{r}\bar{\Omega}+L\frac{\partial \bar{v}}{\partial \bar{z}},\bar{w}=0,\bar{T}=\bar{T}_w,\bar{C}=\bar{C}_w \text{ at } \bar{z}=0, \tag{7}$$

$$\bar{u}\to 0,\bar{v}\to 0,\bar{T}\to\bar{T}_\infty,\bar{C}\to\bar{C}_\infty \quad \text{as } \bar{z}\to\infty, \tag{8}$$

where, $\nu = \mu / \rho_f$ is the kinematic viscosity, μ is the dynamic viscosity, σ is the electrical conductivity of the fluid, ρ is the density, ρ_f is the density of the base fluid, $(\rho c)_p$ is the effective heat capacity of nanoparticles, $\alpha = k/(\rho c)_f$ is the thermal diffusivity, $(\rho c)_f$ is the heat capacity, $\bar{T}$ is the temperature, $\bar{C}$ is the concentration, D_T is the thermophoretic diffusion coefficient, D_B is the Brownian diffusion coefficient, L is the velocity slip constant, $\bar{T}_w$ is the surface temperature, $\bar{T}_\infty$ is the ambient temperature, $\bar{C}_w$ is the surface concentration, $\bar{C}_\infty$ is the ambient concentration, Q_0 is the heat generation/absorption coefficient and R_0 is the rate of chemical reaction. One can use the variables [23],

$$\begin{aligned} &\bar{u} = \bar{r}\bar{\Omega}\frac{dF(\xi)}{d\xi}, \qquad \bar{v} = \bar{r}\bar{\Omega}G(\xi), \qquad \bar{w} = -\sqrt{2\bar{\Omega}\nu}\,F(\xi), \\ &C(\xi) = \frac{\bar{C}-\bar{C}_\infty}{\bar{C}_w-\bar{C}_\infty}, \quad T(\xi) = \frac{\bar{T}-\bar{T}_\infty}{\bar{T}_w-\bar{T}_\infty}, \qquad \xi = \sqrt{\frac{2\bar{\Omega}}{\nu}}\,\bar{z}. \end{aligned} \tag{9}$$

By incorporating these transformation, (1) is satisfied identically and (2)-(8) takes the form:

$$2\frac{d^3F(\xi)}{d\xi^3} + 2F(\xi)\frac{d^2F(\xi)}{d\xi^2} - \left(\frac{dF(\xi)}{d\xi}\right)^2 + (G(\xi))^2 - \beta\frac{dF(\xi)}{d\xi} = 0, \tag{10}$$

$$2\frac{d^2G(\xi)}{d\xi^2} + 2F(\xi)\frac{dG(\xi)}{d\xi} - 2G(\xi)\frac{dF(\xi)}{d\xi} - \beta G(\xi) = 0, \tag{11}$$

$$\frac{d^2T(\xi)}{d\xi^2} + \Pr\left(\begin{array}{l} F(\xi)\dfrac{dT(\xi)}{d\xi} + N_B\dfrac{dT(\xi)}{d\xi}\dfrac{dC(\xi)}{d\xi} + \\ N_T\left(\dfrac{dT(\xi)}{d\xi}\right)^2 + HT(\xi) \end{array}\right) = 0, \tag{12}$$

$$\frac{d^2C(\xi)}{d\xi^2} + Le\Pr F(\xi)\frac{dC(\xi)}{d\xi} + \frac{N_T}{N_B}\frac{d^2T(\xi)}{d\xi^2} - R_pC(\xi) = 0, \tag{13}$$

$$\begin{aligned} &F(\xi) = 0, \ \frac{dF(\xi)}{d\xi} = \lambda\frac{d^2F(\xi)}{d\xi^2}, \ G(\xi) = 1 + \lambda\frac{dG(\xi)}{d\xi}, \\ &T(\xi) = 1, \ C(\xi) = 1, \ \text{at } \xi = 0, \\ &\frac{dF(\xi)}{d\xi} \to 0, \ G(\xi) \to 0, \ T(\xi) \to 0, \\ &C(\xi) \to 0, \quad \text{as } \xi \to \infty. \end{aligned} \tag{14}$$

Here, β is the magnetic field parameter, λ is the velocity slip parameter, $\Pr$ is the Prandtl number, N_T is the thermophoresis parameter, N_B is the Brownian motion parameter, H is the heat generation/absorption parameter, R_p is the chemical reaction parameter, and Le is the Lewis number. These parameters are defined as follows:

$$\begin{aligned} &\beta = \sqrt{\frac{\sigma B_0^{\,2}}{\rho_f\bar{\Omega}}}, \ \lambda = L\sqrt{\frac{2\bar{\Omega}}{\nu}}, N_B = \frac{(\rho c)_p}{(\rho c)_f}\frac{(\bar{T}_w-\bar{T}_\infty)D_T}{\bar{T}_\infty\nu}, \\ &H = \frac{Q_0}{2\bar{\Omega}\rho c_p}, Le = \frac{\alpha}{D_B}, \ \Pr = \frac{\nu}{\alpha}, \\ &N_T = \frac{(\rho c)_p}{(\rho c)_f}\frac{(\bar{C}_w-\bar{C}_\infty)D_B}{\nu}, R_p = \frac{\nu}{2\bar{\Omega}D_B}R_0, \end{aligned} \tag{15}$$

the dimensionless forms of skin friction coefficient (SFC), local Nusselt number (may evaluated as heat transfer rate, HTR) and local Sherwood number (may looked as mass transfer rate, MTR) are defined as:

$$\begin{aligned} &\sqrt{\mathrm{Re}_{\bar{r}}}\,C_F = \frac{d^2F(0)}{d\xi^2}, \ \sqrt{\mathrm{Re}_{\bar{r}}}\,C_G = \frac{dG(0)}{d\xi}, \\ &\frac{Nu}{\sqrt{\mathrm{Re}_{\bar{r}}}} = -\frac{dT(0)}{d\xi}, \quad \frac{Sh}{\sqrt{\mathrm{Re}_{\bar{r}}}} = -\frac{dC(0)}{d\xi}, \end{aligned} \tag{16}$$

in which $\mathrm{Re}_r = \dfrac{(\bar{\Omega}\bar{r})\bar{r}}{2\nu}$ is the local rotational Reynolds number.

III. Numerical Scheme

The dimensionless system of (10)-(13) subjected to boundary condition given by (14) is non-linear in nature. Therefore, for solution traits firstly, the system is converted in terms of initial value problem. The key substitutions used in this regard are

$$q_2 = F'(\xi), q_3 = q'_2 = F''(\xi), \ q_5 = G'(\xi), \ q_7 = T'(\xi), q_9 = C'(\xi),$$

one can obtain

$$\begin{bmatrix} q'_1 \\ q'_2 \\ q'_3 \\ q'_4 \\ q'_5 \\ q'_6 \\ q'_7 \\ q'_8 \\ q'_9 \end{bmatrix} = \begin{bmatrix} q_2 \\ q_3 \\ \dfrac{(q_2)^2 - 2q_1q_3 - q_4^{\,2} + \beta^2q_2}{2} \\ q_5 \\ q_2q_4 - q_1q_5 + \dfrac{1}{2}\beta^2q_4 \\ q_7 \\ -\Pr\left[q_1q_7 + N_Bq_7q_9 + N_Tq_7^{\,2} + Hq_6\right] \\ q_9 \\ -Le\Pr q_9 + \dfrac{N_T}{N_B}q'_7 + R_pq_8 \end{bmatrix}, \tag{17}$$

$$q_1(0)=0,\ \ q_2(0)=\lambda F''(0),\ \ q_3(0)=F''(0),\\ q_4(0)=1+\lambda G'(0),\ \ q_5(0)=G'(0),\ q_6(0)=1,\ q_8(0)=1. \tag{18}$$

with additional conditions

$$q_2(\infty)=0,\ q_4(\infty)=0, q_6(\infty)=0,\ q_8(\infty)=0, \tag{19}$$

The above mentioned scheme is utilized to report numerical solution while this process the initial guessed valued is screened by means of Newton-Raphson method. The suitable achieved initial guess is used. The impacts of involved parameters are examined and offer through graphs.

IV. Analysis

A Newtonian nanofluid flow brought by rotating disk is considered (as shown in Fig. 1). The rotating flow field is manifested with partial slip effect. The role of heat source/sink is admitted by temperature equation, while the chemical reaction phenomena are taken into account by means of concentration equation. The whole physical problem is modelled mathematically in terms of couple partial differential equations (PDE's). To report numerical solution, these equations are converted in terms of system of first order differential equations with the aid of transformation given in (9). While this process the hidden physical parameters are appeared and given in (15). The rotating flow regime characteristics are offered on these parameters namely, velocity slip parameter, thermophoresis parameter, magnetic field parameter, Brownian motion parameter, heat generation parameter, heat absorption parameter and chemical reaction parameter. Moreover, the influences of Reynolds and Lewis numbers are also identified. To be more specific, to see the impact of these physical parameters and involved fundamental numbers on viscous fluid velocity, temperature and nanoparticle concentration, a computational algorithm is executed. The obtained variations are reported by graphical outcomes. In addition, the influence of these parameters on dimensionless Nusselt and Sherwood numbers are discussed by way of tabular structure. To trace out the variation of viscous fluid velocities ($F'(\xi)$ and $G(\xi)$) via physical parameters namely β and λ, Figs. 2 and 3 are plotted. In detail, Fig. 2 is plotted to examine the impact of β on viscous fluid velocities. It can be seen that the inciting values of β have the decline effect on both $F'(\xi)$ and $G(\xi)$. The higher values of β indirectly activate the participation of resistive force named as Lorentz force. This force opposes the movement of particles with respect to both velocity components $\bar{u}$ and $\bar{v}$ when β is varying positively as a magnetic field parameter so that the $F'(\xi)$ and $G(\xi)$ decrease. The effect of λ on both $F'(\xi)$ and $G(\xi)$ is shown in Fig. 3. It is clear that the both velocities reflect diminishing nature for positive values of λ and the corresponding momentum boundary layer is also affected and admits the decline values. Figs. 4 and 5 are plotted to examine the influence of N_T and $\Pr$ in the absence/presence of applied magnetic field along $\bar{z}$ axis when fluid flow is entertained through rotating disk. To be more specific, Fig. 4 offers the impact of N_T on viscous fluid temperature $T(\xi)$. It is noticed that the fluid temperature is enhanced via increasing values of N_T. This inciting reflection is due to bulk motion of particles from hot region to cold one due to higher values of thermophoretic force by altering N_T. The shifting of particles yields the sparking curves of temperature and hence the associated boundary layer thickness increases. Moreover, it is observed that in the absence of magnetic field effect $(\beta=0)$ the viscous fluid temperature is at moderate mode as compared to MHD case $(\beta\neq 0)$. The temperature varies significantly in the case of non-zero values of β. Physically, on increasing the values of β, the drag force known by Lorentz force increases and offers resistance to fluid particles. The continuous resistive behaviour leads to large production of energy and hence the fluid temperature yields higher values. The impact of Pr on viscous fluid temperature is reported in Fig. 5 for both cases that are hydrodynamic and MHD fluid flow due to rotating disk having angular frequency $\bar{\Omega}$. It is seen for both zero and non-zero values of β, the $T(\xi)$ is decreasing function of Pr as expected. The thermal diffusivity has inverse relation with Pr so that the weak thermal diffusivity is reflected towards fluids having higher values of Pr. Such a weak thermal diffusivity is responsible for the decline values of temperature. Further, it is observed (see Fig. 5) that the $T(\xi)$ remarks larger value for MHD case $(\beta\neq 0)$ as compared to hydrodynamic $(\beta=0)$. The effects of H_g on fluid temperature is reported in Fig. 6 for both zero and non-zero values of β. It is observed that for inciting values of H_g the fluid temperature enhances. Physically, the positive values of H_g produced heat energy, as a result $T(\xi)$ increases. The impact of H_a (heat absorption) on $T(\xi)$ is examined and given by means of Fig. 7. It is noticed that the $T(\xi)$ is decreasing function of H_a because of drop of heat energy due to sink. Figs. 8-10 are used to identify the impact of Le, N_B and R_m on nanoparticle concentration $C(\xi)$. In detail, Fig. 8 depicts the influence of Le on $C(\xi)$. It is seen that for positive values of Le, the nanoparticle concentration shows decreasing behaviour, and the concerned concentration layer decreases as well. In addition, it is noticed that the $C(\xi)$ reflects higher magnitude for MHD fluid flow induced by rotating disk as compared to hydrodynamic one. The nanoparticle concentration is affected significantly via positive values of N_B. Fig. 9 is evident that the higher values of N_B bring decline nature subject to $C(\xi)$ for both zero and non-

zero values of β. This effect is due to inciting values of Brownian force because positive variation in N_B enhances the Brownian force to push fluid particles towards opposite direction of $C'(\xi)$ which yields homogeneity in nanofluid. The variation magnitude is significant for the case of MHD as compared to hydrodynamic one. The remarkable changes in nanoparticle concentration is observed via R_m and given by way of Fig. 10. One can see from this figure that the higher values of R_m corresponds decreasing nature of $C(\xi)$ for both zero and non-zero values of β. The curves for MHD $(\beta \neq 0)$ viscous fluid flow yield by rotating disk claim higher magnitude in contrast to hydrodynamic $(\beta = 0)$ fluid flow regime. In this attempt, the MHD viscous nanofluid flow brought by rotating solid disk in the presence of heat source/sink, slip condition and chemical reaction is examined.

For comparison purpose, we reconsider the problem in the absence of both heat sink/source and chemical reaction that is $H = 0$ and $R_m = 0$, our problem absolutely matches with Hayat et al. [22]. In this work, they studied nanoparticle aspects on viscous fluid flow due to rotating disk along with slip effects numerically. We have compared the variation of both Nusselt and Sherwood numbers with their findings as shown in Tables I and II. One can see from these tables that our finding matches with existing values in a limiting sense. The trifling difference is due to the choice of numerical method used in both attempts. Their values are obtained by building in command in Mathematica, while we have used self-coded algorithm (shooting method with R-K scheme) subject to individualities of chemically reactive species and heat source/sink effects on viscous nanofluid flow induced by solid rotating disk.

V. Graphical Results

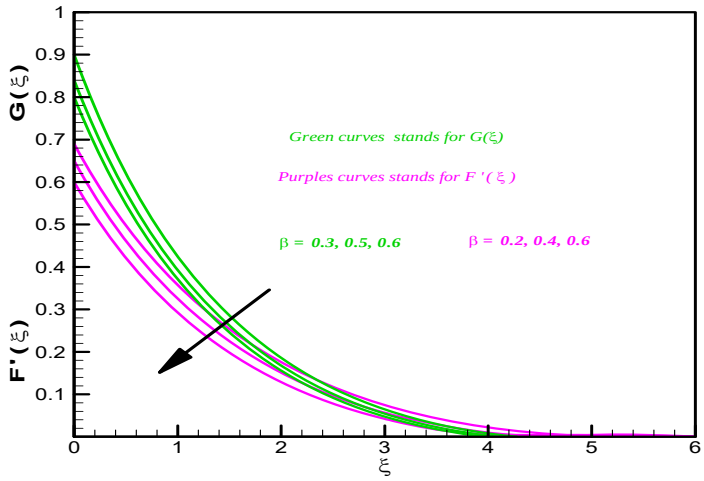

Fig. 2 The impact of β on $G(\xi)$ and $F'(\xi)$

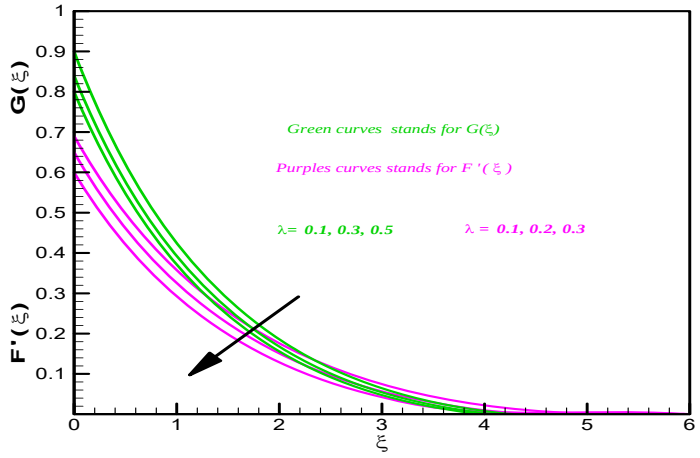

Fig. 3 The impact of λ on $G(\xi)$ and $F'(\xi)$

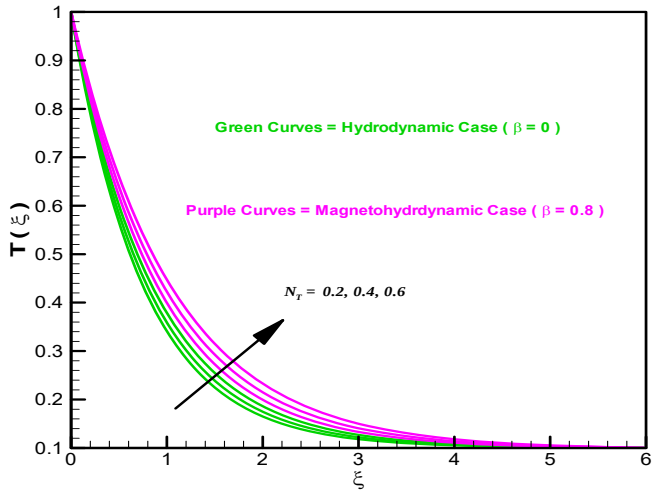

Fig. 4 The impact of N_T on $T(\xi)$

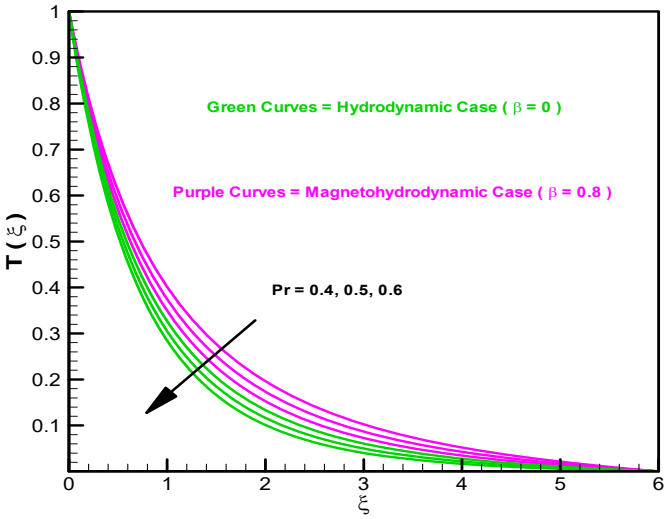

Fig. 5 Impact of Pr on $T(\xi)$

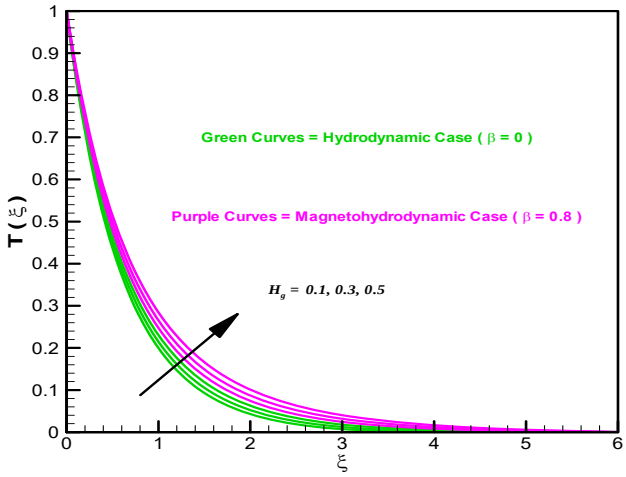

Fig. 6 Impact of H_g on $T(\xi)$

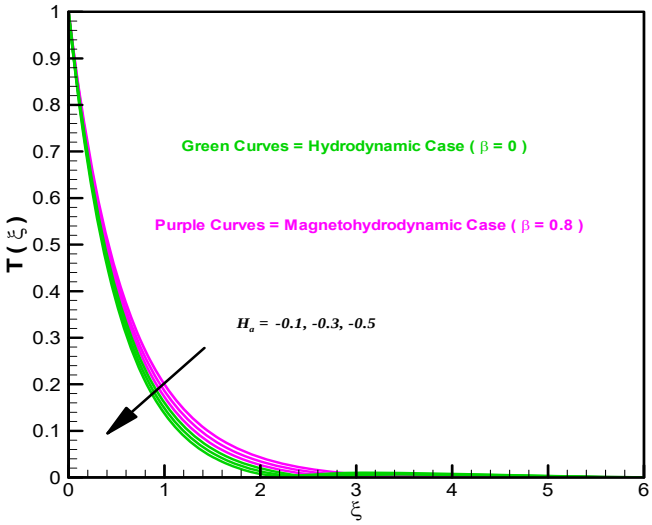

Fig. 7 Impact of H_a on $T(\xi)$

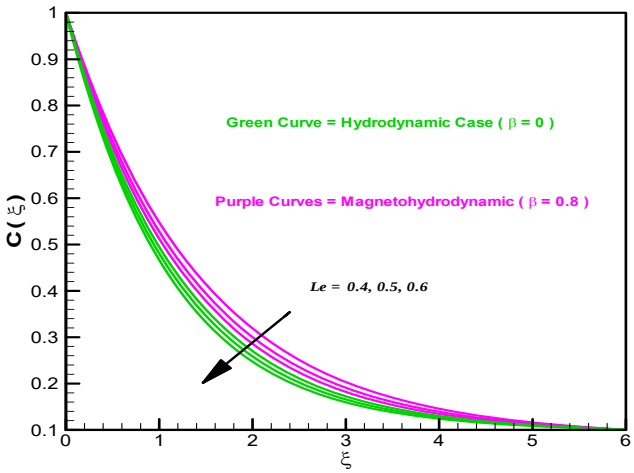

Fig. 8 Impact of Le on $C(\xi)$

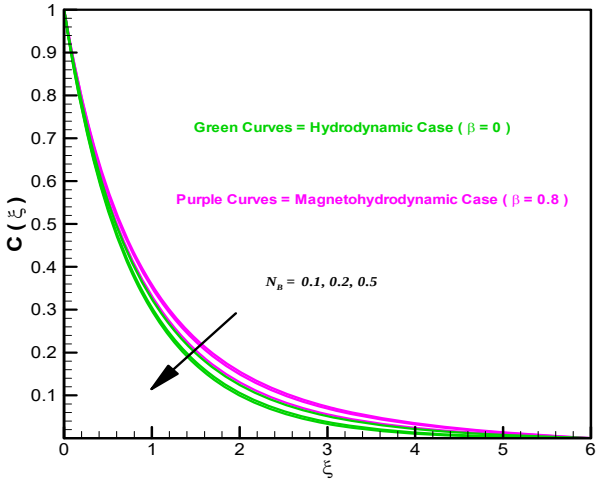

Fig. 9 Impact of N_B on $C(\xi)$

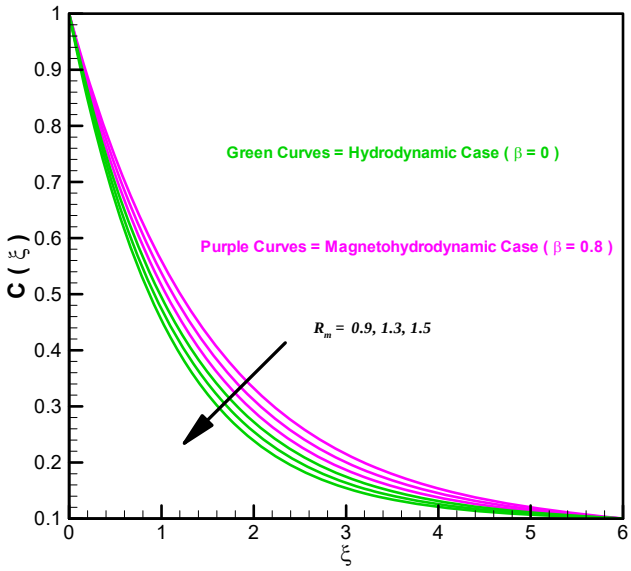

Fig. 10 Impact of R_m on $C(\xi)$

TABLE I
COMPARISON OF HTR WITH EXISTING LITERATURE

λ	β	N_T	Le	Pr	N_B	Hayat et al. [22]	Present values
0.2	-	-	-	-	-	0.32655	0.32660
0.5	-	-	-	-	-	0.30360	0.30363
0.8	-	-	-	-	-	0.28715	0.28724
-	0.0	-	-	-	-	0.30494	0.30502
-	0.7	-	-	-	-	0.24421	0.24434
-	1.4	-	-	-	-	0.17566	0.17572
-	-	0.5	-	-	-	0.25913	0.25915
-	-	0.7	-	-	-	0.23865	0.23878
-	-	1.0	-	-	-	0.21010	0.21024
-	-		0.5	-	-	0.29633	0.29641
-	-		1.0	-	-	0.28954	0.28961
-	-	-	1.5	-	-	0.28395	0.28399
-	-	-	-	0.5	-	0.24989	0.24998
-	-	-	-	1.0	-	0.29211	0.29223
-	-	-	-	1.5	-	0.32286	0.32293
-	-	-	-	-	0.5	0.26341	0.26359
-	-	-	-	-	0.7	0.23677	0.23688
-	-	-	-	-	1.0	0.20056	0.20067

TABLE II
COMPARISON OF MTR WITH EXISTING LITERATURE

λ	β	N_T	Le	Pr	N_B	Hayat et al. [22]	Present values
0.2	-	-	-	-	-	0.27583	0.27591
0.5	-	-	-	-	-	0.26933	0.26942
0.8	-	-	-	-	-	0.26493	0.26499
-	0.0	-	-	-	-	0.27000	0.27011
-	0.7	-	-	-	-	0.25387	0.25395
-	1.4	-	-	-	-	0.23722	0.23734
-	-	0.5	-	-	-	0.22206	0.22212
-	-	0.7	-	-	-	0.22539	0.22561
-	-	1.0	-	-	-	0.22285	0.22286
-	-		0.5	-	-	0.21373	0.21382
-	-		1.0	-	-	0.30132	0.30142
-	-	-	1.5	-	-	0.38690	0.38695
-	-	-	-	0.5	-	0.22934	0.22942
-	-	-	-	1.0	-	0.26624	0.26632
-	-	-	-	1.5	-	0.31262	0.31278
-	-	-	-	-	0.5	0.30338	0.30347
-	-	-	-	-	0.7	0..31875	0..31882
-	-	-	-	-	1.0	0.32959	0.32971

VI. CLOSING REMARKS

A simultaneous way of study is executed numerically to inspect the flow regime characteristics of purely viscous nanofluid flow yield by rotating disk in a both hydrodynamic and MHD frame. The flow field analysis is carried in the presence of pertinent physical effects namely, partial slip, chemical reaction and heat sink/source. The explored key results are itemized as follows:

1. The velocities $F'(\xi)$ and $G(\xi)$ are diminishing function of magnetic field parameter β.
2. Larger values of a slip parameter λ have decline effect on both velocities $F'(\xi)$ and $G(\xi)$.
3. Fluid temperature $T(\xi)$ shows inciting trend towards higher values of thermophoresis parameter N_T.
4. An inciting value of Prandtl number Pr confirms the diminishing nature of fluid temperature $T(\xi)$ for both MHD $(\beta \neq 0)$ and hydrodynamic case $(\beta = 0)$.
5. Fluid temperature $T(\xi)$ shows increasing values for H_g but opposite trend is noticed for the case of H_a.
6. The variations mode of both the $T(\xi)$ and $C(\xi)$ are higher in magnitude for the case of MHD $(\beta \neq 0)$ fluid flow regime as compared to hydrodynamic case $(\beta = 0)$.
7. Nanoparticle concentration $C(\xi)$ is decreasing function of Lewis number Le, Brownian motion and chemical reaction parameters (N_B and R_m).
8. Lower HTR at the surface of rigid disk is noticed via higher values of N_T and N_B.
9. Large MTR is observed at the surface of rigid disk towards positive values of N_T and N_B.

10. Analysis is validated by developing comparison with existing literature which yield the surety of computational algorithm.

ACKNOWLEDGMENT

The authors wish to express their thank to the reviewers for the valuable suggestions to improve the quality of article and also the financial support provided by Higher Education Commission (HEC), Pakistan.

REFERENCES

[1] Chakrabarti A, Gupta AS. Hydromagnetic flow and heat transfer over a stretching sheet. Quarterly of Applied Mathematics. 1979;37(1):73-8.
[2] Andersson HI. An exact solution of the Navier-Stokes equations for magnetohydrodynamic flow. Acta Mechanica. 1995 Mar 1;113(1-4):241-4.
[3] Pop I, Na TY. A note on MHD flow over a stretching permeable surface. Mechanics Research Communications. 1998 May 1;25(3):263-9.
[4] Liao SJ. On the analytic solution of magnetohydrodynamic flows of non-Newtonian fluids over a stretching sheet. Journal of Fluid Mechanics. 2003 Jul;488:189-212.
[5] Sajid M, Hayat T. The application of homotopy analysis method for MHD viscous flow due to a shrinking sheet. Chaos, Solitons & Fractals. 2009 Feb 15;39(3):1317-23.
[6] Fang T, Zhang J, Yao S. Slip MHD viscous flow over a stretching sheet–an exact solution. Communications in Nonlinear Science and Numerical Simulation. 2009 Nov 30;14(11):3731-7.
[7] Fang T, Zhang J. Closed-form exact solutions of MHD viscous flow over a shrinking sheet. Communications in Nonlinear Science and Numerical Simulation. 2009 Jul 31;14(7):2853-7.
[8] Rashidi MM. The modified differential transform method for solving MHD boundary-layer equations. Computer Physics Communications. 2009 Nov 30;180(11):2210-7.
[9] Ghotbi AR. Homotopy analysis method for solving the MHD flow over a non-linear stretching sheet. Communications in Nonlinear Science and Numerical Simulation. 2009 Jun 30;14(6):2653-63.
[10] Kumaran V, Banerjee AK, Kumar AV, Vajravelu K. MHD flow past a stretching permeable sheet. Applied Mathematics and Computation. 2009 Apr 1;210(1):26-32.
[11] Ishak A, Jafar K, Nazar R, Pop I. MHD stagnation point flow towards a stretching sheet. Physica A: Statistical Mechanics and its Applications. 2009 Sep 1;388(17):3377-83.
[12] Kumaran V, Kumar AV, Pop I. Transition of MHD boundary layer flow past a stretching sheet. Communications in Nonlinear Science and Numerical Simulation. 2010 Feb 28;15(2):300-11.
[13] Noor NF, Kechil SA, Hashim I. Simple non-perturbative solution for MHD viscous flow due to a shrinking sheet. Communications in Nonlinear Science and Numerical Simulation. 2010 Feb 28;15(2):144-8.
[14] Tamizharasi R, Kumaran V. Pressure in MHD/Brinkman flow past a stretching sheet. Communications in Nonlinear Science and Numerical Simulation. 2011 Dec 31;16(12):4671-81.
[15] Yang C, Liao S. On the explicit, purely analytic solution of von Kármán swirling viscous flow. Communications in Nonlinear Science and Numerical Simulation. 2006 Feb 28;11(1):83-93
[16] Asghar S, Hanif K, Hayat T, Khalique CM. MHD non-Newtonian flow due to non-coaxial rotations of an accelerated disk and a fluid at infinity. Communications in Nonlinear Science and Numerical Simulation. 2007 Jul 31;12(4):465-85.
[17] Attia HA. Rotating disk flow and heat transfer through a porous medium of a non-Newtonian fluid with suction and injection. Communications in Nonlinear Science and Numerical Simulation. 2008 Oct 31;13(8):1571-80.
[18] Rashidi MM, Shahmohamadi H. Analytical solution of three-dimensional Navier–Stokes equations for the flow near an infinite rotating disk. Communications in Nonlinear Science and Numerical Simulation. 2009 Jul 31;14(7):2999-3006.
[19] Devi SA, Devi RU. Soret and Dufour effects on MHD slip flow with thermal radiation over a porous rotating infinite disk. Communications in Nonlinear Science and Numerical Simulation. 2011 Apr 30;16(4):1917-30.
[20] Dandapat BS, Singh SK. Two-layer film flow over a rotating disk. Communications in Nonlinear Science and Numerical Simulation. 2012 Jul 31;17(7):2854-63.
[21] Turkyilmazoglu M, Senel P. Heat and mass transfer of the flow due to a rotating rough and porous disk. International Journal of Thermal Sciences. 2013 Jan 31;63:146-58.
[22] Hayat T, Muhammad T, Shehzad SA, Alsaedi A. On magnetohydrodynamic flow of nanofluid due to a rotating disk with slip effect: A numerical study. Computer Methods in Applied Mechanics and Engineering. 2017 Mar 1;315:467-77.
[23] Kármán TV. Über laminare und turbulente Reibung. ZAMM-Journal of Applied Mathematics and Mechanics/Zeitschrift für Angewandte Mathematik und Mechanik. 1921 Jan 1;1(4):233-52.